FEASIBILITY STUDY OF INTENSE BEAM MATCHING AT THE SPIRAL INFLECTOR USING ELLIPTICAL SOLENOID

A. Goswami*, P. Sing Babu and V. S. Pandit
Variable Energy Cyclotron Centre, 1/ AF, Bidhannagar, Kolkata-700 064, India

Abstract

A solenoid magnet with elliptical pole face aperture creates unequal focusing forces in the two transverse planes and thus can be utilized for beam matching with unequal sizes as required by spiral inflector for efficient transmission. In this work the beam optical properties of an elliptical solenoid have been studied, including the effect of space charge. An envelope model has been developed and utilized to study the feasibility of using an elliptical solenoid for transverse matching of an intense beam to the acceptance of a spiral inflector.

INTRODUCTION

The injection system of 10 MeV-5 mA proton cyclotron [1] being developed at VECC consists of a 2.45 GHz (80 keV) microwave ion source and two solenoids to transport and match the beam at the spiral inflector [2]. An elliptical solenoid [3] will be placed just before the inflector for transverse matching of the beam. In an elliptical solenoid the elliptic apertures at both ends generate transverse field components which result in unequal focusing forces in two transverse planes. This asymmetric focusing characteristic can be utilized for matching of an intense axisymmetric beam to the spiral inflector, requiring unequal phase ellipses in both planes [2]. In this paper, we have derived the equations of motion in canonical form in the combined linear self-field and applied magnetic field of the elliptical solenoid and obtained a set of envelope equations for uniform density beam. We have modelled a small magnet and computed the magnetic field using a 3D code which is then used in the envelope equations to study the beam optical properties of the magnet. We have also performed detailed study for transverse matching of an axisymmetric intense beam to the input of the spiral inflector.

THEORY

Let an intense continuous beam of particles of charge q and mass m propagating through an elliptical solenoid with an axial momentum $P = m\gamma\beta c$, where β and γ are the relativistic parameters and c is the speed of light. In the laboratory frame, we use a Cartesian coordinate system x, y and z. Here $s = z$ is the distance along the axial direction and x, y are the transverse coordinates from the beam axis. Under paraxial approximation, the components of the magnetic field can be expressed as [3]

$$B_x(x,y,s) = -\big(B_s'(s) - D(s)\big)x/2 \tag{1a}$$

$$B_y(x,y,s) = -\big(B_s'(s) + D(s)\big)y/2 \tag{1b}$$

$$B_s(x,y,s) = B_s(s) \tag{1c}$$

where $B_s(s)$ and $B'_s(s)$ are the field and its derivative on the axis of the solenoid. Here $D(s)$ is related to the field gradient along x and y directions and depends on the elliptic cross-section of the solenoid.

The dimensionless Hamiltonian H for transverse motion of particles in the applied field of the elliptical solenoid and self-field of the beam is given by

$$H = -\frac{qA_s}{P} + \frac{1}{2}\left[\left(p_x - \frac{qA_x}{P}\right)^2 + \left(p_y - \frac{qA_y}{P}\right)^2\right] + \phi^S \tag{2}$$

where p_x and p_y are transverse canonical momentum and H is normalized to $\gamma m\beta^2 c^2$. Here $\phi^S = q\phi/(m\gamma^3\beta^2 c^2)$ is the normalized space charge potential. The components of the vector potential **A** can be obtained by using the gauge $xA_x + yA_y = 0$, which yield $A_x(s) = -B_s(s)y/2$, $A_y(s) = B_s(s)x/2$ and $A_s(s) = D(s)xy/2$. Using the components of the vector potential, the Hamiltonian in Eq. (2) can be expressed as

$$H = -Jxy + \frac{1}{2}\left[(p_x + Ky)^2 + (p_y - Kx)^2\right] + \phi^S \tag{3}$$

where $K = qB_s/(2m\gamma\beta c)$, $J = qD/(2m\gamma\beta c)$ are functions of s. The equations of motion of a particle can be easily derived from the Hamiltonian (3) as

$$x' = p_x + Ky \quad , \quad p_x' = Jy - K^2x + Kp_y - \frac{\partial\phi^S}{\partial x}$$

$$y' = p_y - Kx \quad , \quad p_y' = Jx - K^2y - Kp_x - \frac{\partial\phi^S}{\partial y} \tag{4}$$

where all the variables are function of s. We assume a uniform density beam (KV distribution) with elliptical symmetry. The space charge potential ϕ^S will depend on the spatial elements of the beam matrix $\boldsymbol{\sigma}$ viz σ_{11}, σ_{33} and σ_{13} that is, on the size and orientation of the beam ellipse where for a continuous beam, the $\boldsymbol{\sigma}$ matrix defines the shape of a 4D hyper-ellipsoid $\hat{\mathbf{x}}^T\boldsymbol{\sigma}^{-1}\hat{\mathbf{x}} = 1$. Here $\hat{\mathbf{x}} = (x, p_x, y, p_y)^T$ represents the canonical variables and the "T" denotes the transpose of matrix. The potential ϕ^S in the coordinate system (x, y, s) can be written as [4]

*animesh@veccal.ernet.in

ISBN 978-3-95450-128-1

$$\phi^S(x,y,s) = -\frac{Q}{2}(\phi_{xx}x^2 - 2\phi_{xy}xy + \phi_{yy}y^2), \quad (5)$$

$$\phi_{xx} = \frac{\tilde{r}_x + \tilde{r}_y - (\tilde{r}_x - \tilde{r}_y)\cos 2\theta}{\tilde{r}_x\tilde{r}_y(\tilde{r}_x + \tilde{r}_y)}, \quad \phi_{xy} = \frac{(\tilde{r}_x - \tilde{r}_y)\sin 2\theta}{\tilde{r}_x\tilde{r}_y(\tilde{r}_x + \tilde{r}_y)},$$

$$\phi_{yy} = \frac{\tilde{r}_x + \tilde{r}_y + (\tilde{r}_x - \tilde{r}_y)\cos 2\theta}{\tilde{r}_x\tilde{r}_y(\tilde{r}_x + \tilde{r}_y)} \quad (6)$$

where $Q = qI/(2\pi\varepsilon_0 mc^3\beta^3\gamma^3)$ is the beam perveance, $I = qn_0\pi\tilde{r}_x\tilde{r}_y\beta c$ is the beam current. Here $\tilde{r}_x$, $\tilde{r}_y$ are the beam sizes in the rotated frame $(\tilde{x},\tilde{y},s)$ that is rotated by an angle θ with respect to the s axis and are given by [4]

$$\tilde{r}_x(s) = \frac{1}{\sqrt{2}}\sqrt{\Sigma_S + \Sigma_M}, \quad \tilde{r}_y(s) = \frac{1}{\sqrt{2}}\sqrt{\Sigma_S - \Sigma_M},$$

$$\theta(s) = \frac{1}{2}\tan^{-1}\left(\frac{2\sigma_{13}(s)}{\Sigma_D}\right) \quad (7)$$

where $\Sigma_S = \sigma_{11}(s) + \sigma_{33}(s)$, $\Sigma_D = \sigma_{11}(s) - \sigma_{33}(s)$,

$$\Sigma_M = \sqrt{\Sigma_D^2 + 4\sigma_{13}^2(s)} \quad (8)$$

These beam sizes $\tilde{r}_x(s)$ and $\tilde{r}_y(s)$ and angle $\theta(s)$ have been used in Eq. (6) to determine the self-field potential.

The transverse beam sizes and projected emittances in the laboratory coordinate system can be calculated by using beam matrix $\boldsymbol{\sigma}$ as a function of axial distance s. The evolution of $\boldsymbol{\sigma}$ can be described by [5]

$$\boldsymbol{\sigma}'(s) = \mathbf{F}(s)\boldsymbol{\sigma}(s) + \boldsymbol{\sigma}(s)\mathbf{F}^T(s) \quad (9)$$

where $\mathbf{F}(s)$ specifies the forces acting on the particle and can be obtained by writing the equations of motion (4) in matrix form as $\hat{\mathbf{x}}'(s) = \mathbf{F}(s)\hat{\mathbf{x}}(s)$. Eq. (9) gives ten independent first order equations for the non-zero sigma matrix elements that can be numerically solved to obtain beam size and emittance in x plane (similar in y plane) as

$$r_x(s) = \sqrt{\sigma_{11}(s)}, \quad \varepsilon_x(s) = \sqrt{\sigma_{11}(s)\sigma_{22}(s) - \sigma_{12}^2(s)} \quad (10)$$

RESULTS AND DISCUSSIONS

The injection system at VECC consists of a microwave ion source (protons at 80 keV) and two solenoids S1 and S2 for transport and matching the beam [6]. The location of the spiral inflector is ~ 90 cm from the second solenoid. We need to put an elliptical solenoid between the second solenoid and the spiral inflector for matching.

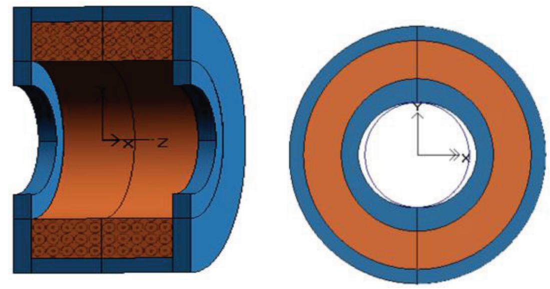

Figure 1: Half 3D model and entrance pole face of the elliptical solenoid.

In the numerical calculation we have modelled a small elliptical solenoid (shown in Fig. 1) and obtained the magnetic field using a 3D code MagNet [7].The magnet has a total length of 15 cm. The semi major and semi minor axes of the elliptic pole face of the solenoid are chosen 6 cm and 5.5 cm respectively to have smaller beam size in y plane as required in our application.

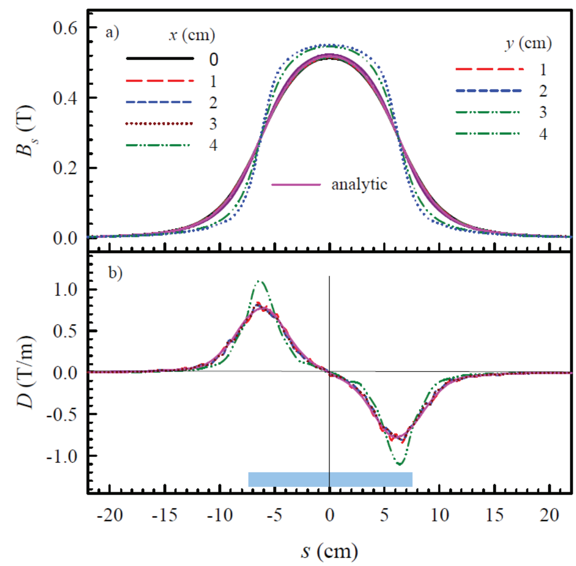

Figure 2: Plots of axial magnetic field B_s and parameter D as a function of s at different values of x and y.

Figure 2 shows the variation of the axial magnetic field $B_s(s)$ and parameter $D(s)$ at different values of transverse coordinates x and y for 29500 A-turn. It is easy to notice that deviation in $B_s(s)$ and $D(s)$ is almost negligible up to the radius of 3 cm. Here $D(s)$ is calculated by subtracting the field gradients evaluated using the fields $B_x(x)$ and $B_y(y)$ at different x and y. In the simulation, we have used the smooth analytical function for $B_s(s)$ and $D(s)$ obtained by fitting the calculated data at 29500 A-turn. The total drift length is 150 cm and the magnet centre is at s_0 = 60 cm from starting point s = 0.

Figure 3 show the evolution of beam envelopes and transverse projected emittances for I = 10 mA at 80 keV injection energy. The input beams are $X(0)$ = $Y(0)$ = 0.5 cm, $X'(0)$ = $Y'(0)$ = 0 mrad and $\varepsilon_x(0)$ = $\varepsilon_y(0)$ = 60 π mm mrad. The beam envelopes in both planes, shown in Fig. 3(a), are different because of $J(s)$ which causes an extra gain in focusing force in the y plane and a reduction

ISBN 978-3-95450-128-1

in the x plane. As a result the beam waist in y plane is formed at a shorter distance s = 113 cm (dotted line) compared to the x plane. Figure 3(b) shows the evolution of the projected emittances. The inter-plane coupling causes increase in the projected emittances in both planes. Their magnitudes are always equal at all the points downstream.

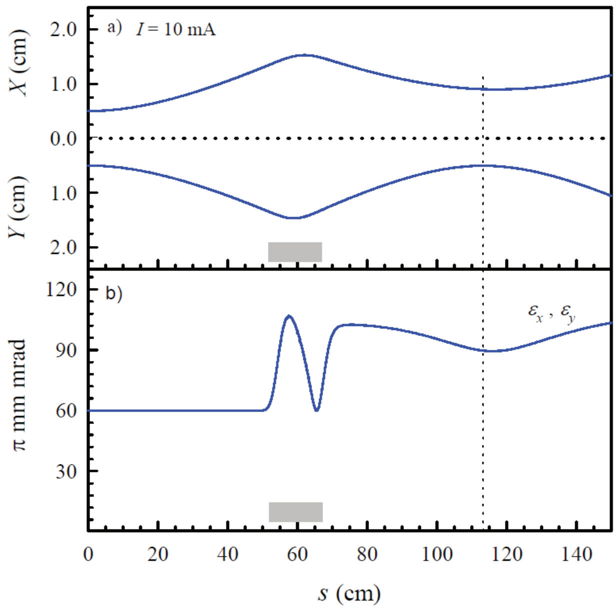

Figure 3: Evolution of (a) beam envelopes and (b) projected emittances for I = 10 mA at 80 keV proton.

In Fig. 4 we have plotted the behaviour of projected emittances through the elliptical solenoid when the initial emittances are unequal in magnitude in the two transverse planes with $\varepsilon_x(0) = 70\ \pi$ mm mrad, $\varepsilon_y(0) = 50\ \pi$ mm mrad and $X(0) = 0.5$ cm, $Y(0) = 0.25$ cm. We see that there is an exchange of emittances from one phase plane to the other phase plane. The projected emittance reduces in the plane where the initial emittance is high. It grows in the other plane where the initial emittance is low. The emittances are always unequal except at a point (as shown by the dotted line) where emittances are equal in both planes. This exchange of emittances is only due to the unequal emittances in the two planes at the input.

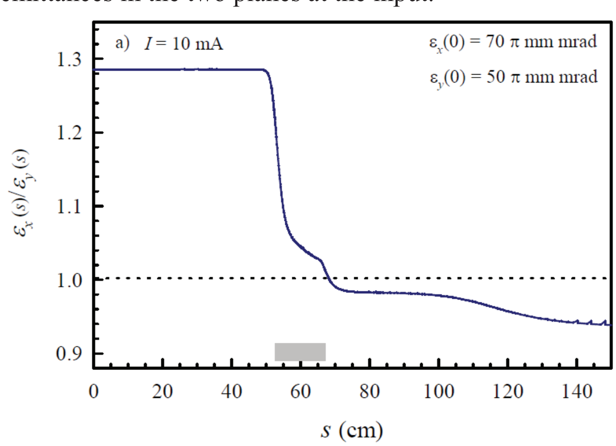

Figure 4: Evolutions of transverse projected emittances obtained at I = 10 mA for non-axisymmetric input beam.

Simulation results on a spiral inflector indicate that convergent phase ellipses with different orientations and a comparatively smaller width in the y plane gives better beam transmission through the spiral inflector. In order to transform the axisymmetric beam to a non-axisymmetric beam for matching at the entrance of the inflector we are planning to use an elliptical solenoid. Figure 5 shows the simulation results of transverse matching of an axisymmetric beam at the entrance of the spiral inflector. The resulting phase ellipses producing a beam of unequal sizes in x and y directions are shown by solid lines in Fig. 5. The required phase ellipses at the entrance of the spiral inflector are shown by dashed curves. The initial beam parameters at the waist position of second solenoid are $X(0) = Y(0) = 0.25$ cm and $\varepsilon_x(0) = \varepsilon_y(0) = 60\ \pi$ mm mrad. The optimized current in the elliptical solenoid is 26000 A-turn and the location of elliptical solenoid and matching point from the beam waist of the second solenoid are 25 cm and 70 cm respectively.

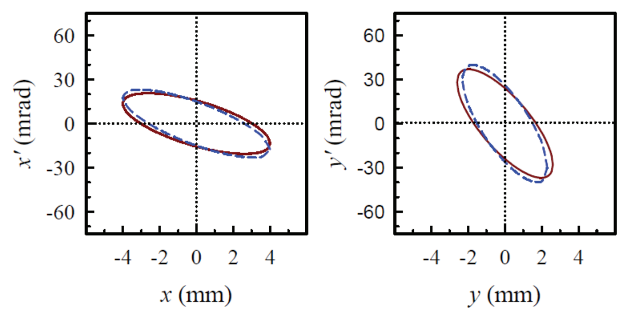

Figure 5: Phase ellipses in the x and y planes for matching at the inflector entrance with average current I = 5 mA.

CONCLUSIONS

In this paper, we have derived beam envelope equations to investigate the focusing and transport of uniformly distributed (KV) space charge dominated beam propagating through the elliptical solenoid. We have studied the emittance growth that results from the coupling between the two transverse planes for different input beam conditions. It is shown that the elliptical solenoid can be used for transverse matching of the beam to the spiral inflector which requires unequal phase ellipses in the two transverse planes.

REFERENCES

[1] A. Goswami, P. Sing Babu and V. S. Pandit, Euro. Phys. Jour. Plus 127 (2012) 47.
[2] A. Goswami, P. Sing Babu and V. S. Pandit, Nucl. Instr. and Meth.A 693 (2012) 276.
[3] A. Goswami, P. Sing Babu and V. S. Pandit, Nucl. Instr. and Meth.A 685 (2012) 46.
[4] A. Goswami, P. Sing Babu and V. S. Pandit, Phys. of Plasmas 19 (2012) 123105.
[5] F. J. Sacherer, Ph.D. thesis, University of California, Berkeley, 1968.
[6] V.S. Pandit, P. Sing Babu, A. Goswami et al., Nucl. Instr. and Meth.B, http://dx.doi.org/10.1016/j.nimb.2013.07.022.
[7] MagNet User Guide, Infolytica Corporation, ver. 6.26.

ISBN 978-3-95450-128-1